SUPPLEMENTARY INFORMATION: PALYNOLOGY AND GEOCHEMISTRY DATA AND METHODS, AND SECTION AGE MODEL

Palynology methods and data

Pollen processing

Pollen processing followed a modified version of the pollen procedures of van der Kaars (1991).

Addition of marker pollen

Lycopodium spore tablets from batch number 938934 (with an average 10, 680 *Lycopodium* spores per tablet) were dissolved in beakers with 10ml of distilled water by heating on hotplates.

Deflocculation

Tetra-sodium pyrophosphate was added to disaggregate the pollen sample (Fægri and Iversen, 1989). Individual samples were placed into beakers alongside 40ml of 10% concentrated tetra-sodium pyrophosphate ($Na_4P_2O_710H_2O$) and heated for 30 minutes.

Sieving

Most pollen ranges in size between 7 and 125µm (Kneller, 2009), and most pollen grains from anemophilous angiosperms range from 20 to 40µm (Jarzen and Nichols, 1996). Therefore samples were sieved through an 8µm nylon mesh.

Calcium carbonate removal

Calcium carbonate was removed using 10% Hydrochloric acid (HCl), and the samples were left to settle overnight. The supernatant liquid was poured off, and the organic materials were transferred to test tubes. The samples were water washed twice by adding distilled water, and centrifuging at 3000 rpm for 5 minutes.

Density separation

The distilled water was decanted, and 4ml of sodium polytungstate with a density of 2.0 was added to float the organic fractions, after which samples were centrifuged at 2500 rpm for 30 minutes. The organic materials were transferred into new test tubes and the inorganics discarded. The organic materials were washed twice in distilled water.

Acetolysis

Acetolysis mixture was used to remove non-pollen organogenic materials. To dehydrate the samples prior to acetolysis, the distilled water was poured off and samples were centrifuged in 6ml of glacial acetic acid at 3000rpm for 5 minutes. Acetolysis mixture contained 9ml of acetic anhydride and 1ml of sulphuric acid. Samples were then heated at 100°C for 5 minutes, followed by centrifuging at 3000rpm for 5 minutes, and sequential washes in glacial acetic acid and distilled water followed with centrifuging after each wash.

Mounting

The chemicals were poured off and 6ml of ethanol was added and centrifuged at 3000rpm for 5 minutes. The ethanol was poured off. Samples were transferred to a small vial, and centrifuged at 3000rpm for another 5 minutes. The mounting medium glycerol was added to the sample residue in a ratio of 3:1. Approximately 2-4 drops of the glycerol solution was placed onto microscopic slides, and the coverslips were sealed with nail varnish.

Pollen Counting

Pollen was counted under a Leica DM500 light microscope, at 400-600X magnification. Pollen grains were compared with online reference collections including the Australasian Pollen and Spore Atlas (APSA Members, 2007), the Newcastle Pollen Collection (Hopf et al., 2005) and New Zealand fossil spores and pollen: an illustrated catalogue (Raine et al., 2008).

Pollen was identified to the lowest taxonomic level possible. A minimum of 100 pollen grains were counted per sample. In ideal circumstances, at least 300 pollen grains would have been counted, however due low concentration of pollen grains in the samples this was not achievable. Charcoal concentrations were determined by counting all black, angular, opaque particles larger than ~5µm encountered in five evenly spaced transects across the slide (Wang et al., 1999).

Pollen and charcoal concentrations per gram (Table DR1) were calculated from count data using the equation

$$C_t = \left(\frac{\left(\frac{T_c}{L_c}\right) \times L_s}{Wt_s} \right)$$

where C_t is the concentration of the target (pollen or charcoal), $\frac{Tc}{L_c}$ is the ratio of taxa counts to *Lycopodium* counts in the slide, L_s is the number of *Lycopodium* grains added to the full sample and Wt_s is the weight of the sample.

Pollen and charcoal counts are presented in Table DR1.

Table DR1. Pollen and charcoal concentration counts (grains per gram)

Palynology sample VM	Geochemistry equivalent	Section height (m)	Charcoal /g	Pollen /g
VM1		-2	1805	18
VM2	Bdst062	6.8	5853	124
VM3	Bdst061	13	2881	123
VM4	Bdst063	20.25	10601	594
VM5	Bdst064	31.5	8577	125
VM6		39	15289	956
VM7		42	14537	557
VM8		50	25082	567
VM9	Bdst069	56	30119	737
VM10		61.5	48405	1111
VM11		67.5	28665	1415
VM12		84	16478	1591
VM13		89	36443	2915
VM14		107.5	117929	3276
VM15	Bdst022	111	185994	4904
VM16		140	44503	2207
VM17	Bdst031	160	41968	1534
VM18		166.4	27091	1944
VM19		171	28178	1953
VM20		178	87863	1196
VM21		183.5	26263	1715
VM22		189.5	29189	2045
VM24		240	9818	661
VM25		237.5	29780	932
VM26		232	21825	2087
VM27		231	46012	2314
VM28		228	47407	2455
VM29		216.6	26631	1446
VM30	Bdst047	212	22649	2290
VM31		203.5	58419	2272

Statistical analysis of pollen data

Three pollen diagrams, a complete taxa diagram (Fig. DR1), a charcoal and pollen concentration diagram (Fig. DR2) and a summarised diagram (Fig 2, main text), were created for the Viqueque Megasequence using the software package Psimpoll version 4.27 (Bennett, 2009). In Figure DR1 all taxa except those with trace values (i.e. taxa whose occurrence was 3 grains or less in their most frequent occurrence) are presented. The removal of these very rare taxa had little effect on the final zonation. Sample VM – 1 was removed from the summary pollen diagram in the main text because the very low pollen count (19 pollen grains) was deemed to be unreliable and produced an artificial peak in Poaceae.

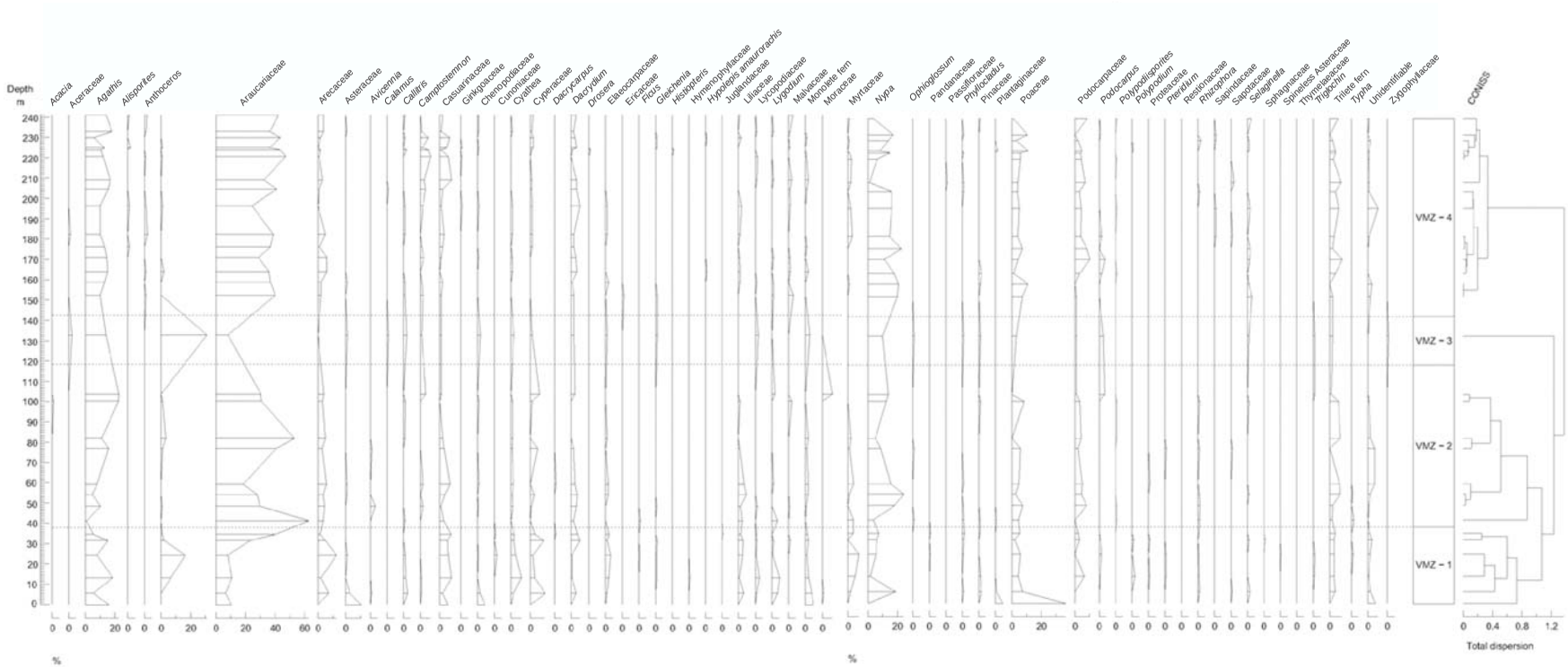
Depth
m
Acacia
Aceraceae
Agathis
Alisporites
Anthoceros
Araucariaceae
Arecaceae
Asteraceae
Avicennia
Callitris
Calytris
Camptostemmon
Casuarinaceae
Ginkgoaceae
Chenopodiaceae
Cunoniaceae
Cyathea
Cyperaceae
Daecrycarpus
Dacrydium
Drosera
Elaeocarpaceae
Ericaceae
Ficus
Gleichenia
Histiopteris
Hymenophyllaceae
Hypolepis amaurorachis
Juglandaceae
Liliaceae
Lycopodiaceae
Lygodium
Malvaceae
Monolete fern
Moraceae
Myrtaceae
Nypa
Ophioglossum
Pandanaceae
Passifloraceae
Phyllocladus
Pinaceae
Plantaginaceae
Proteaceae
Podocarpaceae
Podocarpus
Polycolpites
Polypodium
Proteaceae
Pteridium
Restionaceae
Rhizophora
Sapindaceae
Sapotaceae
Selaginella
Sphagnaceae
Spheleles Asteraceae
Thymelaeaceae
Trigonchin
Trilete fern
Typha
Unidentifiable
Zygophyllaceae
CONISS
VMZ - 4
VMZ - 3
VMZ - 2
VMZ - 1
%
%
Total dispersion

Fig. DR1: (previous page) A pollen diagram for the Viqueque Megasequence with including all taxa with at least a count of three grains on one level. Zonation is derived from CONISS within Psimpoll. Pollen types are in alphabetic order.

Zonation

Zonation based on cluster analysis was performed (Figs. DR1 and DR2). Subdivision of a pollen diagram into zones allows sections of similar fossil content to be grouped, and therefore, patterns of change through time to be identified. The pollen record was zoned using constrained cluster analysis by sum-of-squares (CONISS) as an option within Psimpoll (Bennett, 2009). CONISS clusters sample levels that are highly similar but is constrained to stratigraphically adjacent samples for division (Grimm, 1987).

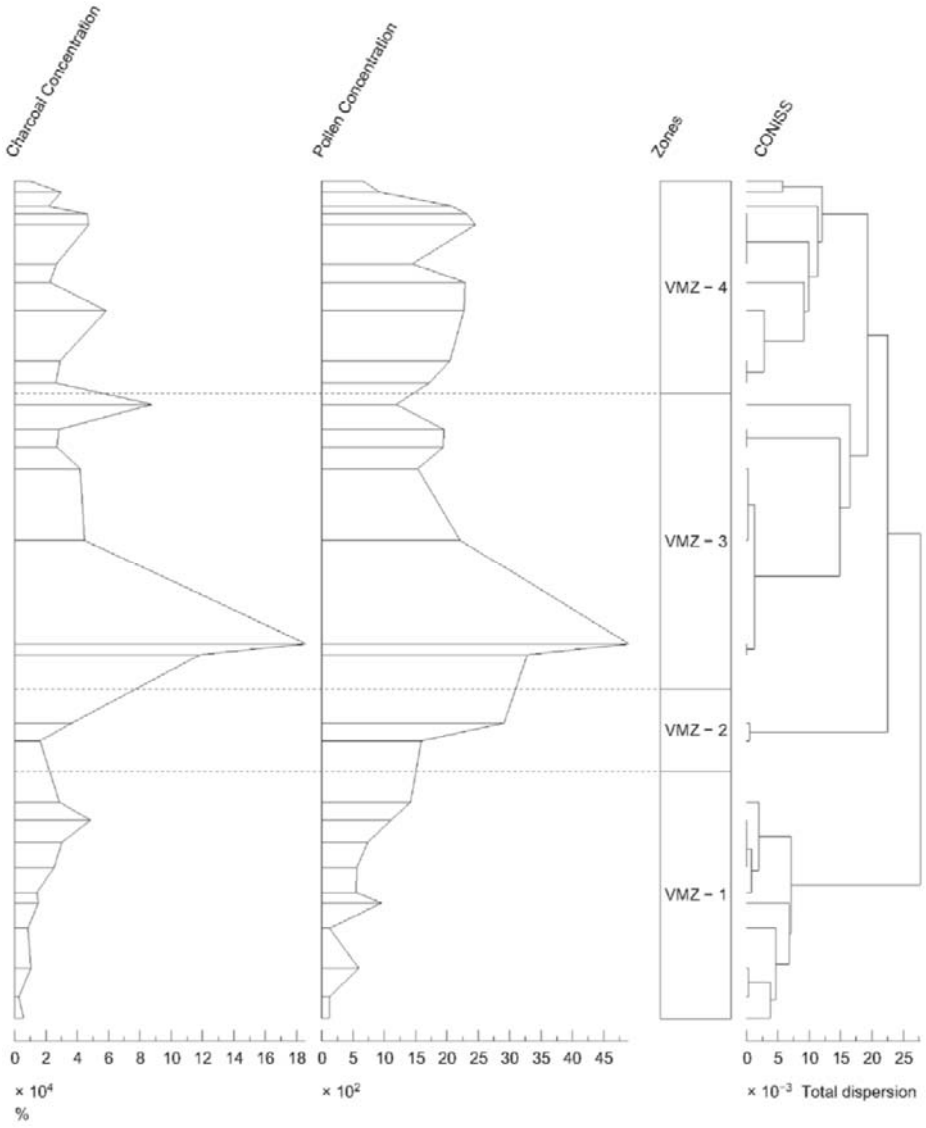

Fig. DR2: Summarised pollen concentration and charcoal diagram.

Principal Component Analysis

Principal component analysis (PCA) is a multivariate analytical method that defines dimensionality in data sets (e.g. Abdi & Williams, 2010). The first principal component represents the strongest trend in the data, and axes thereafter are constrained to be orthogonal to the previous axis (Abdi & Williams, 2010). Three PCA analyses were performed using Canoco version 4.5 (ter-Braak & Smilauer, 2002) to visualize trends in the data.

PCA1: All taxa

The first PCA analysis included all taxa and had numerous rare taxa clustered at the centre of the chart (Fig. DR3). Araucariaceae (7) form the principal axis but the overall diagram is very noisy.

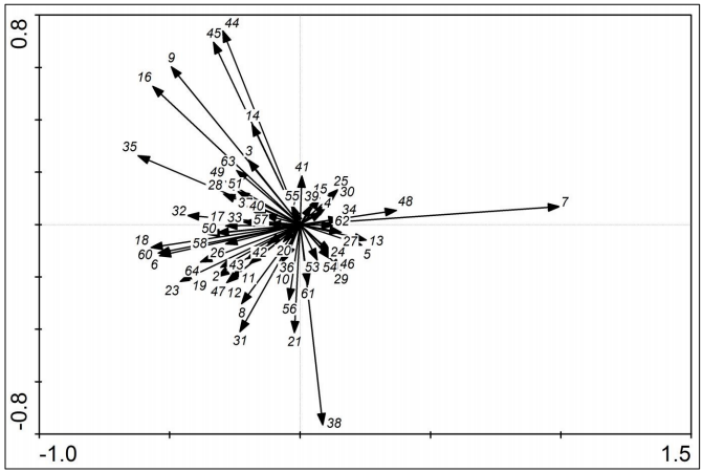

Fig. DR3: Principal Component Analysis for species of all taxa for VM pollen record. Species code 1 *Acacia* (Mimosaceae); 2 Aceraceae; 3 *Agathis*; 4 *Alisporites* (Gymnospermopsida); 5 *Anthoceros* (Anthocerotaceae); 6 *Araucaria*; 7 Araucariaceae; 8 Arecaceae; 9 Asteraceae; 10 *Avicennia*; 11 *Calamus*; 12 *Callitris* (Cupressaceae); 13 *Camptostemon schultzii* (Bombacaceae); 14 Casuarinaceae; 15 Ginkgoaceae; 16 Chenopodiaceae; 17 Cunoniaceae; 18 *Cyathea*; 19 Cyperaceae; 20 *Dacrycarpus*; 21 *Dacrydium*; 22 *Drosera* (Droseraceae); 23 Elaeocarpaceae; 24 Ericaceae; 25 *Ficus* (Moraceae); 26 *Gleichenia* (Gleicheniaceae); 27 *Histiopteris* (Dennstaedtiaceae); 28 Hymenophyllaceae; 29 *Hypolepis amaurorachis* (Dennstaedtiaceae); 30 Juglandaceae; 31 Liliaceae; 32 Lycopodiaceae; 33 *Lygodium* (Schizaeaceae); 34 Malvaceae; 35 Monolete fern; 36 Moraceae; 37 Myrtaceae; 38 *Nypa fruticans* (Arecaceae); 39 *Ophioglossum* (Ophioglossaceae); 40 Pandanaceae; 41 Passifloraceae; 42 *Phyllocladus*; 43 Pinaceae; 44 Plantaginaceae; 45 Poaceae; 46 Podocarpaceae; 47 *Podocarpus*; 48 *Polypodiisporites* (Polypodiaceae); 49 *Polypodium* (Polypodiaceae); 50 Proteaceae; 51 *Pteridium* (Dennstaedtiaceae); 52 Restionaceae; 53 Rhizophora; 54 Sapindaceae; 55 Sapotaceae; 56 *Selaginella* (Sellaginaceae); 57 Sphagnaceae; 58 Spineless asteraceae; 59 Thymelaeaceae; 60 *Triglochin* (Juncaginaceae); 61 Trilete fern; 62 *Typha* (Typhaceae); 63 Unidentifiable; 64 Zygophyllaceae.

PCA2: Summarised Taxa, Excluding Sample VM - 1

The second PCA analysis excluded rare species and combined pteridophytes such as Lycopodiaceae and Cyatheaceae into a single category of 'Ferns' [sic] to reduce noise. Sample VM – 1 was also removed from the second PCA analysis due to low pollen counts which produced a bias toward Poaceae based on the very low count in this sample. This PCA analysis again highlighted Araucariaceae on the first principal component but the rest of the

axes are subdued (Fig. DR4). The percentage of variation accounted for by the first principal component (horizontal axis) of the PCA analysis is 51.2%.

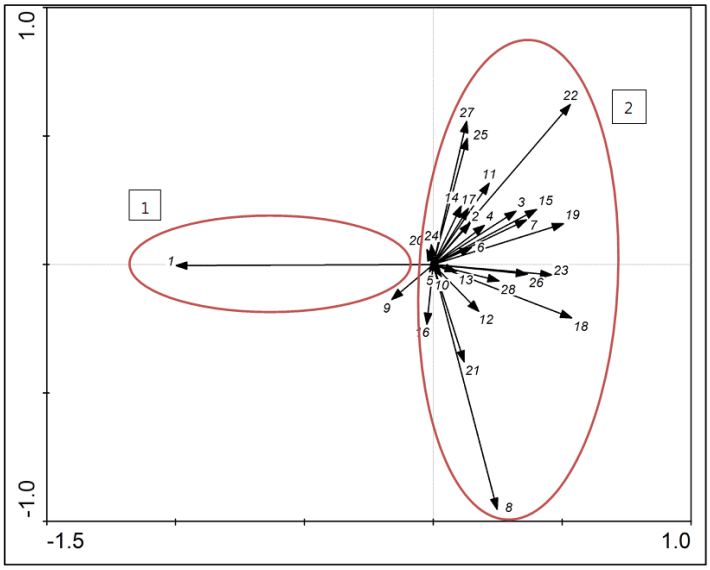

Fig. DR4: PCA species analysis of summarised taxa, excluding sample VM – 1 for the Cuha River, Viqueque Megasequence. Species code: 1 – Araucariaceae, 2 – *Agathis*, 3 – Podocarpaceae, 4 – Pinaceae, 5 – *Alisporites*, 6 – *Callitris*, 7 – Arecaceae, 8 – *Nypa*, 9 – *Camptostemon*, 10 – *Rhizophora*, 11 – *Triglochin*, 12 – *Avicennia*, 13 – Moraceae, 14 – Cunoniaceae, 15 – Elaeocarpaceae, 16 – Sapindaceae, 17 – Sapotaceae, 18 – Asteraceae, 19 – Cyperaceae, 20 – Plantaginaceae, 21 – Poaceae, 22 – Ferns, 23 – Liliaceae, 24 – Malvaceae, 25 – Myrtaceae, 26 – Chenopodiaceae, 27 – Casuarinaceae, 28 – Unidentifiable.

PCA3: Summarised Taxa, Excluding VM – 1 and Araucariaceae

A third PCA analysis was performed on the summarised taxa, excluding sample VM- 1 and Araucariaceae counts (apart from *Agathis* pollen grains). This was undertaken to explore trends that were hidden from the previous analysis by the dominance of the Araucariaceace. The first and second principal components of species (Fig. DR5) of the third PCA are equivalent to the second and third principal component of the second PCA. This analysis allows swamp-mangrove (box 1), lowland forest (box 2), sclerophyll forest (box 3) and less convincingly, lowland rainforest (box 4) to be distinguished.

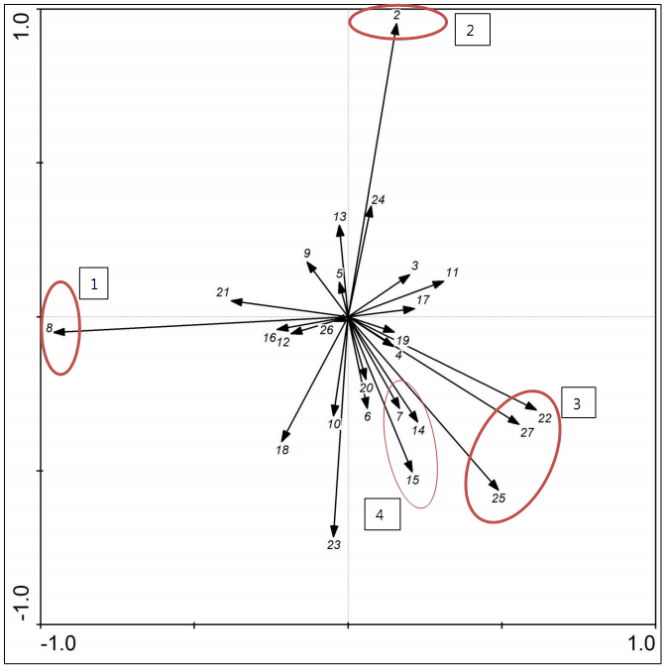

Fig. DR5: PCA species analysis for summarised taxa, excluding VM – 1 and the taxa Araucariaceae for the Cuha River, Viqueque Megasequence. Boxes 1-4 represent mangrove, lowland forest, sclerophyll forest and lowland rainforest respectively. Species code: 2 – *Agathis*, 3 – Podocarpaceae, 4 – Pinaceae, 5 – *Alisporites*, 6 – *Callitris*, 7 – Arecaceae, 8 – *Nypa*, 9 - *Camptostemon*, 10 – *Rhizophora*, 11 – *Triglochin*, 12 – *Avicennia*, 13 – Moraceae, 14 – Cunoniaceae, 15 – Elaeocarpaceae, 16 – Sapindaceae, 17 – Sapotaceae, 18 – Asteraceae, 19 – Cyperaceae, 20 – Plantaginaceae, 21 – Poaceae, 22 – Ferns, 23 – Liliaceae, 24 – Malvaceae, 25 – Myrtaceae, 26 – Chenopodiaceae, 27 – Casuarinaceae.

Geochemistry methods and data

Samples from the type section were analysed to determine weight loss on ignition, major and trace element geochemistry and XRD mineralogy. Loss on ignition (LOI) refers to the weight loss of a sample following combustion in a furnace and is dependent on temperature and duration of combustion. Different temperatures of combustion affect different changes in the composition of the sediment. Loss on ignition at 550°C (LOI_{550}) is generally considered to be proportional to the total organic carbon content of the sediment (Dean, 1974) but may also be contributed to by the loss of structural water in clay, which may account for <20% weight loss in clay rich samples (Mook and Hoskin, 1982; Santisteban et al., 2004). Although total organic carbon generally has a mixed marine/continental signature (e.g. McKirdy and Cook, 1980, DSDP 262), the LOI_{550} stratigraphy in a section is sensitive to changes in depositional setting, particularly as part of an integrated study that incorporates mudstone geochemistry. The dominant factor that causes weight loss in carbonates between 550-1,000°C (reported as LOI_{1000}) is the loss of carbonate CO_2, such that carbonate content can be estimated from LOI_{1000}. When this relationship is used, carbonate estimation error is proportional to clay content and inversely proportional to carbonate content (Santisteban et al., 2004). Wt % carbonate calculated from LOI for clay rich rocks should therefore be viewed with caution.

Loss on ignition

Samples of 12-15 g were air dried and ground to powder in a Rocklabs tungsten carbide ring mill. The samples were oven dried for a minimum of 24 hours at 105°C to remove water and achieve a stable dry weight. The dried powder was decanted into pre-weighed porcelain crucibles. The filled crucibles were reweighed to determine dry weight (DW_{105}) then burnt for exactly two hours at 550°C in a thermostat-controlled Barnstead Thermolyne 1400 muffle furnace. The weight percentage organic carbon was estimated as the weight loss on ignition at 550°C (LOI_{550}), which was calculated following Heiri et al. (2001) as:

$$LOI_{550} = \left(\frac{DW_{105} - DW_{550}}{DW_{105}}\right) \times 100$$

where DW_{105} and DW_{550} are the sample weights before and after burning at 550°C respectively.

X-ray fluorescence spectrometry

The ashed LOI samples were used to produce XRF samples, which were analyzed at the University of Canterbury Geological Sciences Department using a Phillips PW2400 Sequential Wavelength Dispersive X-ray Fluorescence Spectrometer. The spectrometer is calibrated using sets of international standards which have been certified.

Rock majors including SiO2, TiO2, Al2O3, Fe2O3T, MnO, MgO, CaO, Na2O, K2O, and P2O5 were analysed by fused disc. Glass fusion beads were prepared by fusing together approximately 1.3g of rock powder with 6.98g of flux (Li2B4O7 and Li2O mixture) and a few grains of oxidant (NH4NO3) at 1130 ˚C for at least 15 minutes in Pt/Au crucibles. Loss on ignition was calculated after fusion. Glass beads were formed by pouring the molten material into Pt/Au moulds which are cooled rapidly (for rock majors analysis).

Trace elements were analysed by pressed powder pellet. The 32mm diameter pressed powder pellets were prepared using approximately 8g of rock powder and polyvinyl alcohol solution as a binder. The pellets are pressed in a hardened steel die at 3000 psi for 10 seconds.

XRD analysis

Duplicate samples were ground in an agate mortar and pestle with the addition of ethanol to form a slurry. The slurry was transferred to half a microscope slide as a thin layer (orientated mount) using a disposable pipette and allowed to dry at room temperature. The mineralogy of crystalline components of the samples was determined using a Philips PW1729 X-ray generator (50kV/40mA), equipped with a PW2273/20 long fine focus 2.2kW Cu anode x-ray tube, a PW 1820 goniometer, a PW1752 monochromator, a PW1711 sealed gas (Xe) filled proportional detector and a PW1710 diffractormeter control connected to a PC. The PC was loaded with Visual XRD controller software and Traces (V4) search-match software using the Hanawalt search-match algorithm. Peak areas of each identified phase were measured to estimate relative amounts. The samples were scanned from 3° to 70° 2θ with a step size of 0.02° 2θ and scan speed of 0.02° 2θ per second. For determination of swelling/expanding clay mineral content, the air dried slides were placed into a desiccator with ethylene glycol solution overnight in an oven at 60˚C. Once the slides had cooled to room temperature they were scanned from 3° to 30° 2θ. For clay minerals affected by heat the glycolated slides were placed into a muffle furnace for one hour at 550˚C. Once the slides had cooled to room temperature they were scanned from 3 to 30 ° 2θ.

Collated geochemistry data is presented in Table DR2.

Table DR2. Geochemistry results

Sample No:	TS060	TS062	TS061	TS063	TS064	TS069	TS011	TS018	TS022	TS027	TS031	TS035	TS042	TS047
Pollen sample:		vm2	vm3	vm4	vm5	vm9		vm12	vm15		vm17			vm30
Section height	0.1	7	13	20.5	31.5	56	71.5	89	111	139	160	176	197	212.5
						Major elements wt%								
SiO_2	5.57	18.97	26.35	33.14	28.71	47.18	50.6	43.59	42.26	42.09	43.94	49.69	48.27	55.14
TiO_2	0.06	0.26	0.34	0.4	0.39	0.72	0.77	0.66	0.61	0.65	0.68	0.76	0.73	0.87
Al_2O_3	1.39	5.61	7.09	8.51	7.69	13.51	12.03	12.95	12.4	11.39	11.85	15.3	13.51	15.28
Fe_2O_3	0.6	2.32	3	3.63	3.61	6.53	5.66	6.75	7.44	6.25	4.94	7.68	8.5	6.44
MnO	0.07	0.11	0.07	0.09	0.1	0.17	0.13	0.82	0.83	0.28	0.15	0.24	0.51	0.16
MgO	0.46	1.51	2.26	1.93	3.95	3.32	2.74	3.13	3	2.75	2.47	3.13	3.24	3.38
CaO	50.81	38.56	32.13	28.11	27.4	13.14	13.48	15.11	15.88	18.01	17.84	10.25	11.36	7.64
Na_2O	0.16	0.29	0.35	0.75	0.37	1.06	1.21	0.6	0.56	1.03	1.05	1.02	0.95	1.28
K_2O	0.22	0.89	1.16	1.32	1.35	2.3	1.82	2.28	2.27	1.85	1.89	2.46	2.23	2.43
P_2O_5	0.03	0.13	0.13	0.13	0.13	0.15	0.14	0.15	0.17	0.17	0.16	0.16	0.18	0.13
LOI_{550}	1.24	3.31	5.21	6.63	4.54	6.18	4.58	6.48	6.86	4.85	4.47	6.08	7.22	6.14
LOI_{1000}	40.23	30.56	25.8	20.49	25.2	10.89	11.14	13.43	14.02	14.66	14.48	8.89	10.07	6.93
						Roser and Korch (1988) discriminant function values								
R&K F1	-1.06	-1.94	-1.49	-2.08	-0.15	-2.04	-2.08	-2.79	-3.60	-2.91	-1.61	-3.16	-4.17	-1.66
R&K F2	5.21	4.02	5.61	2.37	11.42	2.92	2.78	2.49	1.62	2.14	2.55	1.20	1.18	2.89
						XRD mineralogy								
Quartz	TR	5	10	10	20	50	50	45	35	45	35	55		60
Albite						10	10	tr	5	5	5	10		10
Calcite	100	95	90	90	80	40	40	55	60	50	60	30		25
Kaolinite						TR	TR	TR	TR	TR	TR	5		5
						Trace elements (ppm)								
V	24	67	84	81	79	144	122	134	119	123	126	152	151	157
Cr	14	76	65	52	84	124	108	138	115	115	120	154	121	132
Ni	9	35	39	44	34	62	50	66	53	41	63	51	42	57
Zn	18	59	74	81	71	107	92	100	89	94	102	103	97	110
Zr	28	64	80	91	88	143	158	128	122	125	133	145	139	168
Nb	3	6	7	7	8	15	15	12	12	13	14	16	14	16
Ba	543	293	232	366	458	373	373	544	355	367	359	425	457	418
La	2.5	20	21	22	18	32	27	24	24	23	19	30	26	29
Ce	14	31	29	32	27	52	46	48	47	39	55	50	53	59
Nd	13	19	43	5	23	31	5	30	10	27	49	34	32	48
Ga	3	7	10	10	11	17	15	17	16	15	15	20	17	19
Pb	2	5	4	6	3	15	13	7	12	10	12	17	13	18
Rb	6	38	50	53	63	108	86	105	104	86	89	121	104	116
Sr	920	1143	1217	1176	1121	681	562	709	693	704	709	444	526	358
Th	0.5	4	2	5	3	10	8	10	11	7	9	13	10	13
Y	7	16	19	21	17	28	27	25	23	24	25	30	28	29

Derivation of Section age model

Ages within the section are assigned based on correlation of our measured section with that of Haig and McCartain (2007) (Fig. DR7A). A maximum age for the top of the section of 2.66 ± 0.14 Ma is adopted from Quigley et al. (2012) based on the similarity and proximity of this section with the Northern Cuha section where that age was obtained. A minimum age of latest N21 is adopted for the top of the section (Haig and McCartain, 2007). Interpolation of these ages within the section (Fig. DR7B) yields minimum and maximum ages for attainment of 1000 m of 2.59 Ma and 3.01 Ma respectively, and 2.2 Ma and 2.79 Ma for attainment of 2000 m.

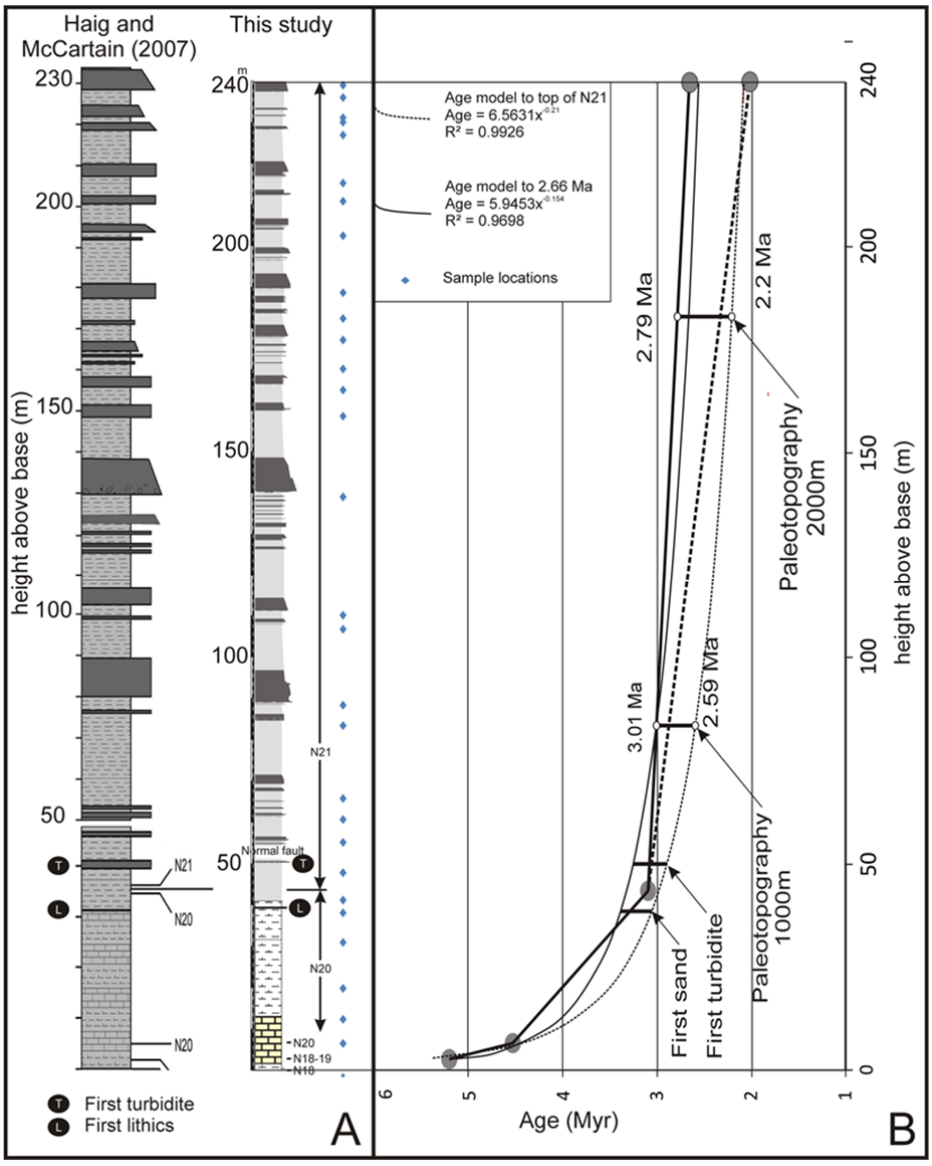

Fig. DR6: A) Correlation of our measured section with that of Haig and McCartain (2007). Note the difference in measured height of beds between the sections. B) Interpolation of ages within section. In order to fully encompass the range of possible uplift rates, ages used are the extreme age selected from options based on punctuated-linear or constant increases in sedimentation rate.

SUPPLEMENTARY REFERENCES

Abdi, H., and Williams, L.J., 2010, Principal Component Analysis, Wiley Interdisciplinary Reviews: Computational Statistics, v. 2, p. 433-459.

APSA Members, 2007, The Australasian Pollen and Spore Atlas, Canberra, Australia, Australian National University.

Bennett, K. D., 2009, Documentation for psimpoll 4.27 and pscomb 1.03. C programs for plotting and analyzing pollen data: The 14Chrono Centre, Archaeology and Palaeoecology.

Dean, W. E., 1974, Determination of carbonate and organic matter in calcareous sediments and sedimentary rocks by loss on ignition: Comparison with other methods: Journal of Sedimentary Petrology, v. 44, p. 242-248.

Fægri, K., and Iversen, J., 1989, Textbook of Pollen Analysis, New York, John Wiley and Sons. Inc, 328 p.:

Grimm, E.C., 1987, CONISS: A FORTRAN 77 program for stratigraphically constrained cluster analysis by the method of incremental sum of squares, Computers & Geoscience, v. 13, p. 13-35.

Haig, D. W., and McCartain, E., 2007, Carbonate pelagites in the post-Gondwana succession (Cretaceous - Neogene) of East Timor: Australian Journal of Earth Sciences, v. 54, no. 6, p. 875-897.

Heiri, O., Lotter, A. F., and Lemcke, G., 2001, Loss on ignition as a method for estimating organic and carbonate content in sediments: reproducibility and comparability of results: Journal of Paleolimnology, v. 25, no. 1, p. 101-110.

Hopf, F., Shimeld, P., and Pearson, S., 2005, The Newcastle Pollen Collection, School of Environmental and Life Sciences at the University of Newcastle, Australia (http://www.aqua.org.au/AQUA/Pollen/).

Jarzen, D. M., and Nichols, D. J., 1996, Pollen, in Jansonius, J., and McGregor, D. C., eds., Palynology: Principles and Applications, Volume 1, American Association of Stratigraphic Palynologists Foundation, p. 261-291.

Kneller, M., 2009, Pollen Analysis, in Gornitz, V., ed., Encyclopedia of Paleoclimatology and Ancient Environments: Netherlands, Springer, p. 815-823.

McKirdy, D. M., and Cook, P. J., 1980, Organic Geochemistry of Pliocene-Pleistocene Calcareous Sediments, DSDP Site 262, Timor Trough: American Association of Petroleum Geologists Bulletin, v. 64, p. 2118-2138.

Mook, D. H., and Hoskin, C. M., 1982, Organic determinations by ignition: Caution advised: Estuarine, Coastal and Shelf Science, v. 15, no. 6, p. 697-699.

Quigley, M.C., Duffy, B., Woodhead, J., Hellstrom, J., Moody, L., Horton, T., Suares, J., and Fernandes, L., 2012, U/Pb dating of a terminal Pliocene coral from the Indonesian Seaway: Marine Geology, v. 311-314, p. 57-62.

Raine, J. I., Mildenhall, D. C., and Kennedy, E. M., 2008, New Zealand Fossil Spores and Pollen: An Illustrated Catalogue, GNS Science (http://www.gns.cri.nz/what/earthhist/fossils/spore_pollen/catalog/index.htm).

Santisteban, J. I., Mediavilla, R., Lopez-Pamo, E., Dabrio, C. J., Blanca Ruiz Zapata, M., Jose Gil Garcıa, M., Castano, S., and Martınez-Alfaro, P. E., 2004, Loss on ignition: a qualitative or quantitative method for organic matter and carbonate mineral content in sediments?: Journal of Paleolimnology, v. 32, p. 287-299.

ter-Braak, C.J.F., and Šmilauer, P 2002, CANOCO Reference manual and CanoDraw for Windows User's guide: Software for Canonical Community Ordination (version 4.5), Microcomputer Power, New York, United States of America.

van der Kaars, W. A., 1991, Palynology of eastern Indonesian marine piston-cores: a Late Quaternary vegetational and climatic record for Australasia: Palaeogeography, Palaeoclimatology, Palaeoecology, v. 85, no. 3-4, p. 239-302.

Wang, X., van der Kaars, S., Kershaw, A.P., Bird, M. and Jansen, F. 1999. A record of fire, vegetation and climate through the last three glacial cycles from Lombok Ridge core G6-4, eastern Indian Ocean, Indonesia. Palaeogeography, Palaeoclimatology, Palaeoecology. v. 147, p. 241-256.